Mathematics and Statistics 11(2): 288-293, 2023 http://www.hrpub.org
DOI: 10.13189/ms.2023.110206

Multivariate Hotelling-T^2 Control Chart for Neutrosophic Data

Saritha M.B, R. Varadharajan*

Department of Mathematics, College of Engineering and Technology, SRM Institute of Science and Technology, Kattankulathur - 603203, Tamil Nadu, India

Received August 7, 2022; Revised January 09, 2023; Accepted February 10, 2023

Cite This Paper in the following Citation Styles

***(a)**: [1] Saritha M.B, R. Varadharajan, "Multivariate Hotelling-T^2 Control Chart for Neutrosophic Data," Mathematics and Statistics, Vol.11, No.2, pp. 288-293, 2023. DOI: 10.13189/ms.2023.110206*

***(b)**: Saritha M.B, R. Varadharajan, (2023). Multivariate Hotelling-T^2 Control Chart for Neutrosophic Data. Mathematics and Statistics, 11(2), 288-293. DOI: 10.13189/ms.2023.110206*

Abstract Industries are consistently confronted with a myriad of challenges, the most significant of which is the requirement to increase product quality while simultaneously minimising manufacturing costs. Statistical Process Control (SPC) provides quality control charts as one of its primary methods for achieving this goal. When it comes to monitoring the quality features of a process, the control chart is the most popular and widely used kind of statistical analysis tool. It is very necessary to make use of multivariate control charts if the quality of a process is found to be connected with more than one characteristic. The Hotelling-T^2 chart is one of the most familiar methods of multivariate control chart. It is used for simultaneously monitoring the process mean and determining whether or not the process mean vector for two or more variables is under control. However, this is applicable only when the data is accurate, determined, and exact. As a result, when the data is vague or ambiguous, the utility of the conventional Hotelling-T^2 control chart is limited. Within the scope of this research, we put up a neutrosophic Hotelling-T^2 control chart as a potential solution to the issue described above. The performance of the proposed chart is evaluated using simulation at various degrees of shift in process average, with the neutrosophic alarm rate serving as the performance measure. To further investigate the applicability of the suggested chart in the actual world, we made use of a real-world example taken from the chemical sector.

Keywords Hotelling-T^2 Control Charts, Neutrosophic Data, Neutrosophic Alarm Rate

1 Introduction

Control charts are the most prevalently employed tool in Statistical Process Control (SPC). It aids in detecting the sources of error by identifying the special and common causes of variations [1]. Univariate control charts have been developed to monitor the quality of a single characteristic. However, in practise, process monitoring and control scenarios incorporate several variables multivariate control charts monitor a number of process variables simultaneously [2]. In many cases, it is necessary to monitor or control two or more significant quality parameters at the same time, but separating these two quality factors can be misleading [3]. Multivariate quality-control challenges are process-monitoring problems with many connected variables. Hotelling (1947) developed multivariate control techniques as a relatively simple way to measure a variety of parameters on each unit of a manufacturing process. However, the nature of the data has experienced numerous changes in recent years. Thus, data need not necessarily to be precise and there is a possibility of indeterminacy. For example, the temperature of a certain city may be high, low or medium and the measurement of the variable data in a complex system may lead to an interval rather than the determined values. In these situations, we also need to consider the indeterminate part of that statement. For dealing with these kinds of indeterminacy in the measurement system, Smarandache [4] developed neutrosophic logic. Neutrosophic Statistics (NS) is an extension of classical statistics, and one deals with set of values instead of crisp values. Applications of neutrosophic logic in variety of fields namely rock measuring, chemical industry, health sector etc [5] -[11]. Aslam and Arif developed Hotelling-T^2 statistic under neutrosophic circumstances, which is the generalization of classical statistics and applied into health care industry for testing purpose [12]. However, here we have been developing neutrosophic Hotelling-T^2 control chart. The primary objective of this study is to deal with indeterminacy in data by employing the Hotelling-T^2 control chart in a generalised form. The theoretical framework of the multivariate Hotelling-T^2 control chart for neutrosophic data has been developed under neutrosophic F distribution with neutrosophic sample size. When there is no indeterminacy in the data, the proposed control chart becomes ordinary Hotelling Control chart with central F distribution.

The remaining portions of the paper are deliberately organized into five sections as follows, section 2 briefly explaines the designing of neutrosphic multivariate Hotelling-T^2 control chart. The neutrosophic alarm rate has been derived in section 3. The performance of the proposed control chart has been studied with the theoretical and simulated alarm rates and the results obtained are depicted in section 4. Furthermore, an illustrative example is provided in section 5. Finally section 6 provides the summary of this study.

2 Designing of Neutrosophic Hotelling-T^2 control chart

Suppose we have k subgroups. And each subgroup has size $n_N \in [\ n_L,\ \ n_U\ ]$
Let

$$\tilde{X}_{ijN} \in \left[\tilde{X}_{ijL}, \tilde{X}_{ijU}\right] = \left[\begin{bmatrix} \tilde{X}_{ij1L} \\ \tilde{X}_{ij2L} \\ \vdots \\ \tilde{X}_{ijpL} \end{bmatrix}, \begin{bmatrix} \tilde{X}_{ij1U} \\ \tilde{X}_{ij2U} \\ \vdots \\ \tilde{X}_{ijpU} \end{bmatrix}\right]$$

denote the jth neutrosophic observation vector on the ith subgroup each having p-components and where i varies from 1 to k.

With out loss of generality let's consider the observations follows neutrospohic multivariate normal distribution, i.e.,

$$\tilde{X}_{ijN} \in \left[\tilde{X}_{ijL}, \tilde{X}_{ijU}\right] \sim N_{pN}\left[[\mu_L\ ,\ \mu_U]\ ,\ [\Sigma_L\ ,\ \Sigma_U]\right] \tag{1}$$

The neutrosophic sample mean vector corresponding to ith subgroup is

$$\bar{\tilde{X}}_{iN} \in \left[\left[\frac{1}{n_L}\sum_{j=1}^{n_L}\tilde{X}_{ijL}\right], \left[\frac{1}{n_U}\sum_{j=1}^{n_U}\tilde{X}_{ijU}\right]\right] = \left[\begin{bmatrix} \bar{\tilde{X}}_{i1L} \\ \bar{\tilde{X}}_{i2L} \\ \cdot \\ \cdot \\ \cdot \\ \bar{\tilde{X}}_{ipL} \end{bmatrix}, \begin{bmatrix} \bar{\tilde{X}}_{i1U} \\ \bar{\tilde{X}}_{i2U} \\ \cdot \\ \cdot \\ \cdot \\ \bar{\tilde{X}}_{ipU} \end{bmatrix}\right] \tag{2}$$

And each

$$\bar{\tilde{X}}_{ijN} \in \left[\bar{\tilde{X}}_{ijL}, \bar{\tilde{X}}_{ijU}\right] \sim N_{pN}\left[[\mu_L\ ,\ \mu_U]\ ,\ \left[\frac{\Sigma_L}{n_L}\ ,\ \frac{\Sigma_U}{n_U}\right]\right]$$

The neutrosophic form of $\bar{\tilde{X}}_{ijN} \in \left[\bar{\tilde{X}}_{ijL}, \bar{\tilde{X}}_{ijU}\right]$ can be written as

$$\bar{\tilde{X}}_{ijN} = \bar{\tilde{X}}_{ijL} + \bar{\tilde{X}}_{ijU}\ I_N; I_N \in [I_L, I_U]$$

Note that $\bar{\tilde{X}}_{ijN} \in \left[\bar{\tilde{X}}_{ijL}, \bar{\tilde{X}}_{ijU}\right]$ is the generalisation of sample mean vector under classical statistics. The data matrix under $\bar{\tilde{X}}_{ijN} \in \left[\bar{\tilde{X}}_{ijL}, \bar{\tilde{X}}_{ijU}\right]$ reduces to sample mean vector under classical statistics when $I_L = 0$. And the corresponding neutrosophic sample covariance matrix of the ith subgroup is

$$\tilde{S}_{iN} \in \left[\tilde{S}_{iL}\ ,\ \tilde{S}_{iU}\right] = \left[\begin{bmatrix} \tilde{S}_{i11L} & \tilde{S}_{i12L} & \dots & \tilde{S}_{i1pL} \\ \tilde{S}_{i21L} & \tilde{S}_{i22L} & \dots & \tilde{S}_{i2pL} \\ . & . & \dots & . \\ \tilde{S}_{ip1L} & \tilde{S}_{ip2L} & \dots & \tilde{S}_{ippL} \end{bmatrix}, \begin{bmatrix} \tilde{S}_{i11U} & \tilde{S}_{i12U} & \dots & \tilde{S}_{i1pU} \\ \tilde{S}_{i21U} & \tilde{S}_{i22U} & \dots & \tilde{S}_{i2pU} \\ . & . & \dots & . \\ \tilde{S}_{ip1U} & \tilde{S}_{ip2U} & \dots & \tilde{S}_{ippU} \end{bmatrix}\right]$$

Now, we can take the estimate of the neutrosophic population mean vector

$$\hat{\mu}_N = [\hat{\mu}_L\ ,\ \hat{\mu}_U] = \bar{\bar{\tilde{X}}}_N \in \left[\left[\frac{1}{k}\sum_{i=1}^{k}\bar{\tilde{X}}_{iL}\right],\ \ \left[\frac{1}{k}\sum_{i=1}^{k}\bar{\tilde{X}}_{iU}\right]\right] \tag{3}$$

And the estimate of the neutrosophic population covariance matrix is

$$\begin{aligned} \hat{\Sigma}_N &= \left[\hat{\Sigma}_L\ ,\ \hat{\Sigma}_U\right] \\ &= \bar{\tilde{S}}_N \in \left[\bar{\tilde{S}}_L\ ,\ \bar{\tilde{S}}_U\right] \\ &= \left[\left[\frac{1}{k}\sum_{i=1}^{k}\tilde{S}_{iL}\right], \left[\frac{1}{k}\sum_{i=1}^{k}\tilde{S}_{iU}\right]\right] \end{aligned} \tag{4}$$

$$\tilde{S}_{ihh'N} \in \left[\left[\frac{1}{n_L-1}\sum_{j=1}^{n_L}\left(x_{ijhL} - \bar{x}_{ihL}\right)\left(x_{ijh'L} - \bar{x}_{ih'L}\right)\right], \left[\frac{1}{n_U-1}\sum_{j=1}^{n_U}\left(x_{ijhL} - \bar{x}_{ihL}\right)\left(x_{ijh'L} - \bar{x}_{ih'L}\right)\right]\right]$$

where $h,\ h' = 1, 2,\ \dots,\ p$. Note that $\tilde{S}_{ihh'N} \in \left[\tilde{S}_{ihh'L},\ \tilde{S}_{ihh'U}\right]$ is the generalization of sample covariance under classical statistics, and the covariance matrix $\tilde{S}_{iN} \in \left[\tilde{S}_{iL}\ ,\ \tilde{S}_{iU}\right]$ reduces to the sample covariance under classical statistics when there is no indeterminacy in the observations.

The corresponding sample correlation matrix $\tilde{r}_{ihh'N} \in \left[\tilde{r}_{ihh'L}\ ,\ \tilde{r}_{ihh'U}\right]$ representing the pairwise correlation coefficient between $X_{ihN} \in [X_{ihL}, X_{ihU}]$ and $X_{ih'N} \in [X_{ih'L}, X_{ih'U}]$ i.e., the hth and h'th components of the ith subgroup of r_{jkN} is given by

$$\tilde{r}_{ihh'N} \in \left[\left[\frac{\tilde{S}_{ihh'L}}{\sqrt{\tilde{S}_{ihhL}\tilde{S}_{ih'h'L}}}\right], \left[\frac{\tilde{S}_{ihh'U}}{\sqrt{\tilde{S}_{ihhU}\tilde{S}_{ih'h'U}}}\right]\right], \tag{5}$$

where, $h, h' = 1, 2, \ldots, p$. Then the neutrosophic form of $\tilde{r}_{ihh'N} \in [\tilde{r}_{ihh'L}\ ,\ \tilde{r}_{ihh'U}]$can be written as

$$\tilde{r}_{ihh'N} = \tilde{r}_{ihh'L} + \tilde{r}_{ihh'U}\ I_N; I_N \in [I_L, I_U]$$

Then the Neutrosophic Hotelling-$T^2{}_N$ statistic is

$$\begin{aligned} T^2_{iN} &\in \left[T^2_{iL}\ ,\ T^2_{iU}\right] \\ &= \left[\left[n_L\left(\bar{\bar{X}}_{iL} - \bar{\bar{X}}_L\right)^T\left(\bar{\bar{S}}_L\right)^{-1}\left(\bar{\bar{X}}_{iL} - \bar{\bar{X}}_L\right)\right],\right. \\ &\left.\left[n_U\left(\bar{\bar{X}}_{iU} - \bar{\bar{X}}_U\right)^T\left(\bar{\bar{S}}_U\right)^{-1}\left(\bar{\bar{X}}_{iU} - \bar{\bar{X}}_U\right)\right]\right] \end{aligned} \tag{6}$$

Since there are more than one observation in the subgroups, it can be shown that.

$$\left[\left[\frac{(kn_L - k - p + 1)}{(k-1)(n_L - 1)p} T^2_{iL}\right], \left[\frac{(kn_U - k - p + 1)}{(k-1)(n_U - 1)p} T^2_{iU}\right]\right] \sim \left[F_{p,(kn_L - k - p + 1),\ \delta_L}\ ,\ F_{p,(kn_U - k - p + 1),\ \delta_U}\right]$$

where

$$\begin{aligned} \delta_N &\in [\delta_L\ ,\ \delta_U] \\ &= \left[\left[n_L\left(\mu_L - \bar{\bar{X}}_L\right)^T\left(\bar{\bar{S}}_L\right)^{-1}\left(\mu_L - \bar{\bar{X}}_L\right)\right],\right. \\ &\left.\left[n_U\left(\mu_U - \bar{\bar{X}}_U\right)^T\left(\bar{\bar{S}}_U\right)^{-1}\left(\mu_U - \bar{\bar{X}}_U\right)\right]\right] \end{aligned} \tag{7}$$

is the neutrosophic non-centrality parameter. Under the null hypothesis, i.e., when actually the process is in control about the target mean vector, the non-centrality parameter becomes zero. So the neutrosophic control limits obtained for the proposed control chart are
$LCL = 0$ and

$$\left[UCL_L = \frac{(k-1)(n_L - 1)p}{(kn_L - k - p + 1)} F(1-\alpha)_{(p,(kn_L - k - p + 1))}\ ,\ UCL_U = \frac{(k-1)(n_U - 1)p}{(kn_U - k - p + 1)} F(1-\alpha)_{(p,(kn_U - k - p + 1))}\right] \tag{8}$$

where $F(\alpha)$ is the α^{th} quantile of neutrosophic F distribution.

3 Neutrosophic Alarm Rate

In the process control environment, the term 'alarm' denotes that a point is out of control limit. It can happen while the process is in control as well the process is not in control. When a point is plotted outside of the control limits during a statistically controlled process, the control chart gives us a deceptive indication that the process is out of control. These signals are known as false alarms, and in order to create the control limits, the false alarm rate is often set at a low level. Whereas the process is out of control, i.e., if there is a shift in the process, the control chart ought to be able to recognise it immediately. Only then can we claim that the control chart is effective. In this paper, we have developed the neutrosophic alarm rate for the multivariate neutrosophic Hotelling-T^2 control chart.

Let us denote

$$F(\alpha)_{(p,(kn_L - k - p + 1))} = a_L\ ,$$
$$F(\alpha)_{(p,(kn_U - k - p + 1))} = a_U\ ,$$
$$F(1-\alpha)_{(p,(kn_L - k - p + 1))} = b_L \quad \text{and}$$
$$F(1-\alpha)_{(p,(kn_U - k - p + 1))} = b_U$$

Then under the null hypothesis, i.e., when the process is in control, the probability of a point outside the control limits is

$$\begin{aligned} &P\left(T^2_{iL} < \frac{(k-1)(n_L - 1)p}{(kn_L - k - p + 1)} a_L\right) \\ &\quad + P\left(T^2_{iL} > \frac{(k-1)(n_L - 1)p}{(kn_L - k - p + 1)} b_L\right) \\ &= P\left(\frac{(kn_L - k - p + 1)}{(k-1)(n_L - 1)p} T^2_{iL} < a_L\right) \\ &\quad + P\left(\frac{(kn_L - k - p + 1)}{(n_L - 1)p} T^2_{iL} > b_L\right) \\ &= 1 - P\left(\frac{(kn_L - k - p + 1)}{(k-1)(n_L - 1)p} T^2_{iL} < b_L\right) \\ &\quad + P\left(\frac{(kn_L - k - p + 1)}{(k-1)(n_L - 1)p} T^2_{iL} < a_L\right) \\ &= 1 - F_{0L}(b_L) + F_{0L}(a_L) \end{aligned}$$

where $F_{0N}(.) \in [F_{0L}(.)\ , F_{0U}(.)]$ is the CDF of neutrosophic central F distribution with degrees of freedoms $p, (kn_L - k - p + 1)$ and $p, (kn_U - k - p + 1)$ respectively.

Now suppose the process mean of the hth component has been shifted m_h times of its standard deviation,the mean of the corresponding component becomes,

$$\left[\left[\bar{\bar{X}}_{hL} + m_h \bar{\bar{S}}_{hhL}\right], \left[\bar{\bar{X}}_{hU} + m_h \bar{\bar{S}}_{hhU}\right]\right]$$

where, h = 1, 2, 3, . . . , p
Then the statistic $\frac{(kn_N - k - p + 1)}{(k-1)(n_N - 1)p} T^2_{iN}$
follows non-central neutrosophic F distribution with parameters p, $(kn_N - k - p + 1)$ and the corresponding non-centrality parameter is

$$\delta_N = n_N (M_N)^T \left(\bar{\bar{S}}_N\right)^{-1} (M_N) \tag{9}$$

where

$$\delta_N \in [\delta_L\ ,\ \delta_U] = \left[\left[n_L (M_U)^T \left(\bar{\bar{S}}_U\right)^{-1} (M_U)\right],\ \left[n_U (M_U)^T \left(\bar{\bar{S}}_U\right)^{-1} (M_U)\right]\right]$$

Table 1. Alarm Rate for limits with an α = 5%. The expected alarm rates have been computed based on the neutrosophic F distribution, and the observed alarm rates are the mean fraction of out-of-control points.

Shift	sample size					
	[4, 6]		[6, 8]		[8, 10]	
	Expected	Observed	Expected	Observed	Expected	Observed
0	[5, 5]	[5.08, 5.47]	[5, 5]	[4.98, 5.04]	[5, 5]	[4.97, 5.04]
0.25	[5.3, 5.4]	[5.13, 5.49]	[5.4, 5.5]	[5.56, 5.61]	[5.5, 5.7]	[5.68, 5.76]
0.5	[6.16, 6.9]	[6.30, 7.31]	[6.9, 7.72]	[7.11, 7.55]	[7.72, 8.61]	[8.13, 9.02]
1	[11.59, 16.53]	[11.52, 16.51]	[16.53, 22.16]	[16.5, 24.51]	[22.16, 28.12]	[23.45, 28.67]
1.5	[24.9, 38.94]	[25.03, 39.28]	[38.94, 52.52]	[40.54, 52.72]	[52.57, 64.56]	[53.98, 65.14]
2	[46.28, 67.83]	[46.78, 68.43]	[67.83, 82.59]	[68.2, 82.77]	[82.59, 91.30]	[83.42, 92.18]
2.5	[69.7, 88.97]	[69.5, 89.32]	[88.97, 96.62]	[88.96, 96.54]	[96.62, 99.09]	[96.78, 99.07]
3	[87.2, 97.71]	[87.12, 97.73]	[97.71, 99.68]	[97.62, 99.80]	[99.68, 99.96]	[99.66, 99.93]

$$M_N \in [M_L\ , M_U]$$
$$= \left[\begin{bmatrix} \bar{\bar{X}}_{1L} + m_1 \bar{\bar{S}}_{11L} \\ \bar{\bar{X}}_{2L} + m_2 \bar{\bar{S}}_{22L} \\ . \\ . \\ . \\ \bar{\bar{X}}_{pL} + m_p \bar{\bar{S}}_{ppL} \end{bmatrix}, \begin{bmatrix} \bar{\bar{X}}_{1U} + m_1 \bar{\bar{S}}_{11U} \\ \bar{\bar{X}}_{2U} + m_2 \bar{\bar{S}}_{22U} \\ . \\ . \\ . \\ \bar{\bar{X}}_{pU} + m_p \bar{\bar{S}}_{ppU} \end{bmatrix} \right]$$
$$- \left[\begin{bmatrix} \bar{\bar{X}}_{1L} \\ \bar{\bar{X}}_{2L} \\ . \\ . \\ . \\ \bar{\bar{X}}_{pL} \end{bmatrix}, \begin{bmatrix} \bar{\bar{X}}_{1U} \\ \bar{\bar{X}}_{2U} \\ . \\ . \\ . \\ \bar{\bar{X}}_{pU} \end{bmatrix} \right]$$
$$= \left[\begin{bmatrix} m_1 \bar{\bar{S}}_{11L} \\ m_2 \bar{\bar{S}}_{22L} \\ . \\ . \\ . \\ m_p \bar{\bar{S}}_{ppL} \end{bmatrix}, \begin{bmatrix} m_1 \bar{\bar{S}}_{11U} \\ m_2 \bar{\bar{S}}_{22U} \\ . \\ . \\ . \\ m_p \bar{\bar{S}}_{ppU} \end{bmatrix} \right]$$

Now the alarm rate becomes,

$$1 - F_{1L}(b_L) + F_{1L}(a_L) \text{ and } 1 - F_{1U}(b_U) + F_{1U}(a_U) \quad (10)$$

where $F_{1N}(.) \in [F_{1L}(.)\ , F_{1U}(.)]$is the CDF of neutrosophic non-central F distribution with dfs $p, (kn_L - k - p + 1)$ and $p, (kn_U - k - p + 1)$ respectively and the non-centrality parameter by (9).

4 Simulation Study

In the previous sections we have derived the expressions for the control limits and alarm rate for the proposed chart based on the neutrosophic F-distribution. A simulation study has been conducted out, so that the effectiveness of theoretical control limits can be assessed. The performance of the proposed control chart in process with under control scenario; In other words, no shift in the process and various levels of shift in the process average has been evaluated with the neutrosophic alarm rate. When the process is in a state of control, the alarm rate should be equal to the nominal value; that is, it should be equal to the pre-planned probability of type I error (false alarm rate) α that is used to derive the control limits. If the process average is shifted to a different value, the alarm rate should be increased according to the magnitude of the shift. For the simulation purpose, we utilised R software (version 4.0.2), a false alarm rate α of 0.05, a number of subgroups of k = 100, and neutrosophic sample size $[n_L,\ n_U]$ = [4, 6], [6, 8] and [8, 10]. The parameters described above have resulted in the generation of data drawn at random from a tri-variate multivariate neutrosophic normal distribution centred around zero. The shift thresholds were chosen to be 0.25, 0.5, 1, 1.5, 2, and 3 standard deviations from the centre, regardless of direction. The predicted alert rate from the neutrosophic F distribution has been derived using equation 3 and the average fraction of out-of-control points has been estimated based on 1000 iterations. The results have been presented in Table 1. Based upon the results of the simulation, it can be observed that the theoretical and observed alarm rates coincide approximately. Moreover, alarm rate increases according to the magnitude of the shift. The sample size also has an effect on the alarm rate; as it grows, the proposed chart can discover the change at a quicker pace.

5 Illustrative Example

To illustrate the proposed control chart, neutrosophic data has been generated following the guidelines provided in [14] with the mean vector and covariance matrix utilised in [15] with the neutrosophic sample size of [3, 5] and the number of subgroups equal to 20. The data for example in [15] come from a chemical procedure, each observation has three components: the percentage of contaminants, the temperature, and the concentration strength. For each subgroup, Table 2 contains the summary statistics (process average of each component and associated neutrosophic T^2 statistic). To determine the control limits, we will also use α = 0.05. As a result of equation 8, the upper control limits of the proposed neutrosophic Hotelling-T^2 control chart are $[UCL_L,\ UCL_U]$ = [7.956, 8.555] and Figure 1 is the corresponding control chart. As none of the plotted $\left[T^2_{iL},\ T^2_{iU}\right]$ values exceed the upper control limits, we can conclude that the process is in a state of statistically in-control.

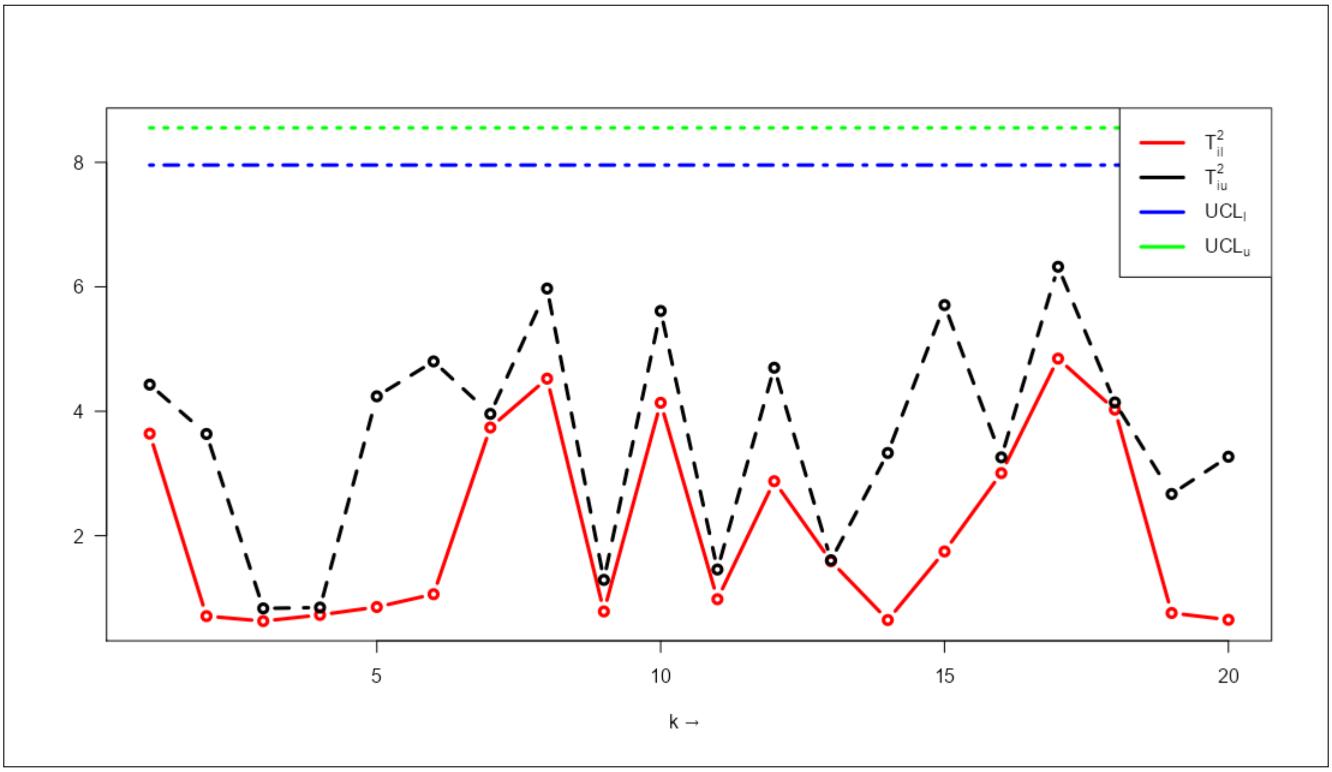

Figure 1. The Neutrosophic Hotelling-T^2 control chart. No out of control points has been detected

Table 2. Summary Statistics of the illustrative example

k	$\left[\bar{\bar{X}}_{i1L}, \bar{\bar{X}}_{i2U}\right]$	$\left[\bar{\bar{X}}_{i2L}, \bar{\bar{X}}_{i2U}\right]$	$\left[\bar{\bar{X}}_{i3L}, \bar{\bar{X}}_{i3U}\right]$	$[T^2_{iL},\ T^2_{iU}]$
1	[17.159, 17.659]	[85.972, 86.155]	[42.496, 42.546]	[3.64, 4.428]
2	[16.55, 16.744]	[83.785, 87.012]	[42.506, 44.201]	[0.708, 3.635]
3	[16.702, 17.231]	[85.823, 85.949]	[42.814, 43.356]	[0.628, 0.832]
4	[16.26, 16.794]	[84.996, 85.611]	[42.907, 42.995]	[0.727, 0.846]
5	[17.558, 18.603]	[85.221, 85.404]	[42.893, 43.13]	[0.854, 4.24]
6	[16.891, 17.19]	[84.79, 84.944]	[43.127, 43.328]	[1.06, 4.801]
7	[17.105, 17.3]	[85.241, 85.278]	[43.058, 43.384]	[3.739, 3.958]
8	[17.168, 17.882]	[83.041, 85.148]	[43.347, 43.517]	[4.524, 5.972]
9	[16.243, 16.916]	[83.45, 84.138]	[42.747, 43.736]	[0.783, 1.29]
10	[16.349, 16.422]	[84.678, 85.635]	[42.641, 43.468]	[4.136, 5.612]
11	[16.969, 17.336]	[85.054, 85.869]	[43.201, 43.706]	[0.98, 1.457]
12	[16.989, 17.181]	[84.736, 86.513]	[43.387, 43.443]	[2.876, 4.7]
13	[16.752, 17.185]	[85.118, 85.789]	[42.681, 42.814]	[1.59, 1.606]
14	[17.159, 17.37]	[82.87, 85.894]	[42.975, 44.143]	[0.645, 3.33]
15	[17.067, 17.379]	[84.571, 86.874]	[42.885, 43.735]	[1.747, 5.707]
16	[16.479, 17.402]	[84.549, 85.986]	[42.914, 42.991]	[3.006, 3.259]
17	[15.921, 16.35]	[85.517, 86.536]	[42.203, 42.985]	[4.846, 6.322]
18	[16.424, 17.531]	[85.282, 85.599]	[43.294, 43.422]	[4.026, 4.142]
19	[16.02, 17.224]	[84.148, 84.786]	[43.21, 43.467]	[0.758, 2.671]
20	[16.758, 16.843]	[84.002, 85.093]	[42.943, 43.266]	[0.649, 3.269]

6 Conclusion and Summary

The traditional approach of Hotelling-T^2 control chart deals only with determined and exact data; when there is indeterminacy in the data, we must also account for it. In this paper, we have developed Hotelling-T^2 control charts in a neutrosophic environment based on the theory of neutrosophic F-distribution. We have used a neutrosophic alarm rate to determine how quickly the proposed control chart will detect an out-of-control point or process shift. In addition, we have conducted a simulation study by introducing a shift in the process, causing the central neutrosophic F-distribution to transform into a noncentral neutrosophic F-distribution with a noncentral parameter δ. Furthermore, the simulation study reveals that the theoretical and simulated outcomes coincide. Finally for the purpose of demonstration, a data from chemical field has been taken and the working of the chart has been illustrated. Moreover, when the data is exact, the proposed control chart reduces to the classical Hotelling-T^2 control chart. Based on our research, we conclude that the proposed chart is applicable for both exact and neutrosophic data.

REFERENCES

[1] Nihal Erginel, Sevil Sentük, Cengiz Kahraman, and Ihsan Kaya, Evaluating the packing process in food industry using fuzzy and [stilde] control charts. International Journal

of Computational Intelligence Systems, 4(4):509–520, 2011.

[2] Nola D. Tracy, John C. Young, Robert L. Mason, ”Multivariate control charts for individual observations”, Journal of quality technology, Vol.24, pp.88-95, 1992, doi.org/10.1080/00224065.1992.12015232

[3] Montgomery, Douglas C. Introduction to statistical quality control. John Wiley & Sons, 2020.

[4] F. Smarandache. Introduction to neutrosophic statistics: Infinite study. Romania-Educational Publisher, Columbus, OH, USA, 2014.

[5] Chen, Jiqian and Ye, Jun and Du, Shigui, ”Scale effect and anisotropy analyzed for neutrosophic numbers of rock joint roughness coefficient based on neutrosophic statistics”, Symmetry, Vol.9, pp.208, 2017, doi.org/10.3390/sym9100208

[6] Jiqian Chen, Jun Ye, Shigui Du, Rui Yong, ”Expressions of Rock Joint Roughness Coefficient Using Neutrosophic Interval Statistical Numbers”, Symmetry, Vol.9, pp.128, 2017, doi.org/10.3390/sym9070123

[7] Aslam, Muhammad, ”Design of Sampling Plan for Exponential Distribution Under Neutrosophic Statistical Interval Method” IEEE Access, Vol.6, pp.64153-64158, 2018, doi.10.1109/ACCESS.2018.2877923.

[8] Aslam, Muhammad and Albassam, Mohammed, ”Application of neutrosophic logic to evaluate correlation between prostate cancer mortality and dietary fat assumption”, Symmetry, Vol.11, pp. 330, 2019, doi.org/10.3390/sym11030330.

[9] Aslam, Muhammad, ”Attribute control chart using the repetitive sampling under neutrosophic system” IEEE Access, Vol.7, pp.15367-15374, 2019, doi.110.1109/ACCESS.2019.2895162.

[10] Aslam, Muhammad, ”Product acceptance determination with measurement error using the neutrosophic statistics”, Advances in Fuzzy Systems, Vol.2019, pp.1-8, 2019, doi.10.1155/2019/8953051.

[11] Aslam, Muhammad and Khan, Nasrullah and Khan, Muhammad Zahir, ”Monitoring the variability in the process using neutrosophic statistical interval method”, Symmetry, Vol.10, pp.562, 2018, doi.org/10.3390/sym10110562.

[12] Aslam, Muhammad and Arif, Osama H, ”Multivariate analysis under indeterminacy: An application to chemical content data”, Journal of Analytical Methods in Chemistry, Vol.2020, pp.6, 2020, doi.org/10.1155/2020/1406028.

[13] Team, R. Core. ”R Core Team: A language and environment for statistical computing R Foundation for Statistical Computing.” Vienna, Austria, 2013.

[14] Pavel Skrabanek, Natalia Martinkova, ”Getting started with fitting fuzzy linear regression models in R”,2019 1992

[15] Tracy, Nola D., John C. Young, and Robert L. Mason., ”Multivariate control charts for individual observations.”, Journal of quality technology, Vol.24, pp.88-95, 1992, doi.org/10.1080/00224065.1992.12015232